Industrial Crops & Products 225 (2025) 120490

Contents lists available at ScienceDirect

Industrial Crops & Products

journal homepage: www.elsevier.com/locate/indcrop

Stepwise degumming of pineapple leaf fibers with tunable fineness and excellent antibacterial property

Shiyu Liao [a], Jianming Chen [a,b], Li Li [c], Puwang Li [d], Xungai Wang [a,b,*]

[a] The Hong Kong Polytechnic University, Joint Research Centre for Fiber Innovations and Renewable Materials, School of Fashion and Textiles, Kowloon, Hong Kong
[b] Research Centre of Textiles for Future Fashion, The Hong Kong Polytechnic University, Kowloon, Hong Kong
[c] Division of Integrative Systems and Design, The Hong Kong University of Science and Technology, New Territories, Hong Kong
[d] South Subtropical Crops Research Institute, Chinese Academy of Tropical Agricultural Sciences, Zhanjiang, Guangdong 524091, China

ARTICLE INFO

Keywords:
Pineapple leaf fibers
Step-by-step degumming
Single fibril
Fineness
Antibacterial properties

ABSTRACT

Pineapple leaf fibers (PALFs) are often disposed of as agricultural waste or byproducts. These fibers have great potential for textile and functional applications due to their high cellulose content, good tensile strength, and excellent antibacterial properties. Degumming is a critical process to remove non-cellulose components, enabling the transformation of PALFs into value-added products. However, traditional one-step alkaline degumming cannot precisely remove target specific gum residues, complicating the control of fiber fineness and promising antibacterial properties. To address these challenges, this study proposed an innovative step-by-step degumming strategy for PALF, termed SSD-PALF in short, which enabled the selective and sequential removal of components such as lignin and hemicellulose. This approach allowed separation of tightly packed fiber bundles into individual ribbon-like fibrils. The ultimate fineness and chemical components of four widely cultivated varieties across the globe were investigated. Furthermore, the proposed SSD-PALF enabled a remarkable reduction in hemicellulose content of Queen PALF from 23.49% to 4.89 %, while preserving over 10 % lignin. Correspondingly, the fiber width decreased significantly, from 45 to 75 μm to 16.7 μm, reflecting a 72.2 % improvement in fineness. It is evident that the fiber fineness can be well regulated through the precise control of hemicellulose ratio within PALF. It is flexible to reduce the fiber fineness by 42 %, 31 % and up to 28 % of its original value according to our stepwise degumming method. Notably, the refined PALF maintained robust antibacterial properties against three bacteria (*S. aureus*, *E. coli* and *C. albicans*), with > 90 % bacteriostatic rate. These findings point to ways of tuning PALF fineness and retaining its functional properties, potentially extending its applications in both textile and non-textile industries.

1. Introduction

Fast fashion has stimulated the rapid development of synthetic fibers from non-renewable petroleum sources, which however poses an adverse impact on the environment and alters people's purchasing behaviors. The market for natural fibers is continuously shrinking as a percentage of total fiber consumption, partly due to the high price commanded by natural fibers. For example, the price of flax fiber has been soaring from US$3.98/kg to US$9.54/kg over the past five years, with an approximately 140 % increase in the first quarter of 2024 (Fibre2Fashion, 2024). This price surge has spurred interest in utilizing free agricultural waste as lignocellulosic materials to develop new functionalities. Pineapple leaf fibers (PALFs), stand out as a promising candidate due to their abundance, low cost, and remarkable mechanical and antibacterial properties (Kengkhetkit and Amornsakchai, 2014; Padzil et al., 2020). Despite these advantages, the utilization of PALF is extremely low, since the majority of pineapple leaves are either buried, burned, or used as livestock feed following the harvest of pineapple fruit, contributing to grave environmental pollution and resource wastage (Sethupathi et al., 2024). Therefore, there is an urgent need to increase the utilization of PALF as an environment-friendly and economically viable natural fiber.

Historically, PALFs have been known as the "white gold from soil" due to their valuable nature, commanding a premium price in the

* Corresponding author at: The Hong Kong Polytechnic University, Joint Research Centre for Fiber Innovations and Renewable Materials, School of Fashion and Textiles, Kowloon, Hong Kong.
E-mail addresses: lesley.liao@connect.polyu.hk (S. Liao), jianming.chen@polyu.edu.hk (J. Chen), lillyli@ust.hk (L. Li), puwangli@163.com (P. Li), xungai.wang@polyu.edu.hk (X. Wang).

https://doi.org/10.1016/j.indcrop.2025.120490
Received 31 October 2024; Received in revised form 11 December 2024; Accepted 5 January 2025
Available online 11 January 2025

market. In the Philippines, it is traditionally used to craft piña fabric, a luxurious textile once presented to Kings and Queens as royal gifts. However, the high labor cost of fiber extraction and hand-weaving processes limited its broader adoption. Furthermore, the lack of refinement techniques hindered its transition to industrial-scale applications. Unlike other natural fibers such as cotton and wool, PALF exists as relatively coarse (~10 times coarser than cotton) and long bundles (up to 90 cm), rather than as individual short fibers (Mukherjee and Satyanarayana, 1986). This is due to its rich gum content, which includes hemicellulose, lignin, pectin, and waxy substances (Triastuti, 2021). Degumming is necessary to separate the fiber bundles into finer, shorter fibers for further processing and end-use applications. For yarn spinning, it has been suggested to control the gum content of bast fibers below 10 % to meet spinning requirement (Yang and Zhang, 1999). In the jute spinning system, the stiffness, brittleness, and hardness of PALF make it difficult to spin into fine yarns (Indra Doraiswamy and Chellamani, 1993), relegating the resultant coarse yarns to agricultural uses (Balbin et al., 2022). Additionally, PALF cannot be easily processed in the cotton spinning system, where the typical linear density of cotton fibers is 1.56–2.12 dtex, considerably lower than that of PALF (~ 13.5–20.7 dtex) (Franck, 2005; Foulk and Mcalister III, 2002). Due to the unclear morphology and characteristics of the ultimate fibrils of PALF, it is challenging to precisely gauge the degree of degumming. This often results in difficulties in simultaneously balancing fiber fineness and length. Given these challenges, careful control of the degumming process is essential to achieve the desired fiber fineness.

Water retting, the earliest method used for degumming is limited in efficiency due to its long processing time and heavy reliance on manual labor (Dey et al., 2021). Biological degumming, despite higher efficiency and lower pollution, presents challenges in adjusting complex degumming conditions such as incubation temperature, pH, and the formation of purified enzymes, resulting in uncontrollable degumming outcomes (Xiang et al., 2019). Alkali degumming processes, which employ highly concentrated alkali solution and auxiliary agents to completely remove all gum components, effectively reduce the gum content and fiber diameter (Indra Doraiswamy and Chellamani, 1993). This method is easier to operate and more efficient compared to water retting and biological degumming. However, the one-step reaction in traditional alkali degumming can be so intense that the antibacterial properties of fibers are inevitably diminished and the fiber fineness is hard to control precisely (Fan et al., 2010). As previously reported, the intrinsic antibacterial properties of fibers could be well preserved if it is able to regulate the degumming process with a gum content above 20 % (Yang and Zhang, 1999). Therefore, the relationship between gum content and PALF's fineness and antibacterial performance needs further investigation.

In addition, unlike similar bast fibers, which are categorized into specific types such as hemp, flax, jute, ramie, and kenaf fibers, research on PALF tends to treat it as a generic category, without distinguishing between the various pineapple fiber varieties. This lack of differentiation presents a significant challenge in the existing literature, as there is considerable variation in the reported properties of PALF. This inconsistency is likely due to factors such as differences in the pineapple plant varieties used (often unspecified), variations in testing conditions, and discrepancies in fiber extraction and degumming methods, all of which impact on fiber dimensions. To address this gap, we selected four widely cultivated pineapple varieties across the globe for a detailed examination of their components, structure, morphology, and ultimate fibrils under the same condition of extraction and degumming. This approach aims to provide a more accurate and comprehensive understanding of PALF as a sustainable material.

In this work, we devised a precise degumming strategy named SSD-PALF that allows for quantitative control over the removal of each component for tunable fiber fineness while maintaining robust antibacterial properties. Specifically, acetone was first used to get rid of the fat, wax, and other water-soluble impurities; Then, ammonium carbonate was added to remove the pectin by chelation; Subsequently, lignin and hemicellulose were tuned using oxidant and alkaline solution, respectively. As a result, the basic structure, components, and ultimate fibril fineness of four typical pineapple varieties were fully determined, providing a comprehensive knowledge of PALFs. Additionally, the characteristics of each gum component in PALF morphology were identified, with the role of hemicellulose in determining fiber fineness highlighted. We effectively refined fibers by controlling hemicellulose residue below 10 %, ensuring PALF uniformity for future industrial production. Finally, the natural antibacterial properties of both raw and degummed PALF were evaluated and compared, demonstrating that refined PALF maintained excellent bacteriostatic rates against bacteria strains (*Escherichia coli* ATCC 8099, *Staphylococcus aureus* ATCC 6538 and *Candida albicans* ATCC 10231), thus laying the foundation for the development of functional PALF textiles or other high value-added products.

2. Experimental section

2.1. Materials and reagents

Materials: Four varieties of raw pineapple leaf fibers (PALFs), denoted as MD-2 PALF from Malaysia (provided by University Putra Malaysia), Smooth Cayenne PALF from Thailand (sourced from Saeng Charoen Grand Co., Ltd), Queen PALF (named Bali in China) and Red Spanish PALF from China (acquired from the pineapple planting base of the South Subtropical Crops Research Institute, CATAS, in Zhanjiang City, Guangdong province), were selected in this study. These raw PALFs are long fiber bundles without any treatment.

Reagents: The chemical reagents used in experiments were acetone (CH_3COCH_3, 99.8 %), ammonium oxalate ($(NH_4)_2C_2O_4$ 98.0 %), aqueous sulfuric acid (H_2SO_4, 95.0 %), barium chloride ($BaCl_2$, 99.0 %), sodium chlorite ($NaClO_2$, 31 % in H_2O), acetic acid (CH_3COOH, 99.0 %), sodium hydroxide (NaOH, 96 %), ammonium hydroxide solution (NH_4OH, 25.0–28.0 %) and absolute ethyl alcohol (C_2H_5OH,99.9 %), purchased from Dieckmann Chemical Industry Co., Ltd., HK; Deionized water (H_2O), deionized by the GenPure Water Purification System, was supplied from the laboratory. All the chemicals were used as received without any further purification.

2.2. Methods

2.2.1. Step-by-step degumming of PALF

The step-by-step degumming (SSD) was designed to selectively remove specific components while minimizing damage to others. This degumming procedure sequentially eliminates fat, wax, water soluble matter, pectin, lignin, and hemicellulose, as depicted in the schematic of PALF refinement (Fig. 1).

In Step 1, acetone, a polar aprotic solvent, was used to remove fat and wax via Soxhlet extraction. As an organic solvent with moderate polarity, acetone effectively dissolves non-polar and weakly polar compounds such as waxes and oils. These compounds, which have long hydrocarbon chains, interact with acetone through van der Waals forces, facilitating their dissolution (Furse et al., 2015). The Soxhlet extraction method enhances this process by continuously cycling the solvent: upon heating, the solvent evaporates, condenses, and flows back through the sample, thereby increasing extraction efficiency. Acetone's low boiling point makes it easy to evaporate and condense, making it well-suited for recycling in Soxhlet extraction equipment.

Following this, step 2 involved the use of ammonium oxalate to convert water-insoluble calcium pectinate into soluble pectin ammonium salt, effectively dissolving the pectin within the fibers (Taylor, 2012). Pectin is a complex polysaccharide primarily composed of galacturonic acid units linked by α-1,4-glycosidic bonds. Pectin molecules contain carboxyl groups (-COOH), which can dissociate in solution to form carboxylate ions ($-COO^-$), providing binding sites for metal ions or

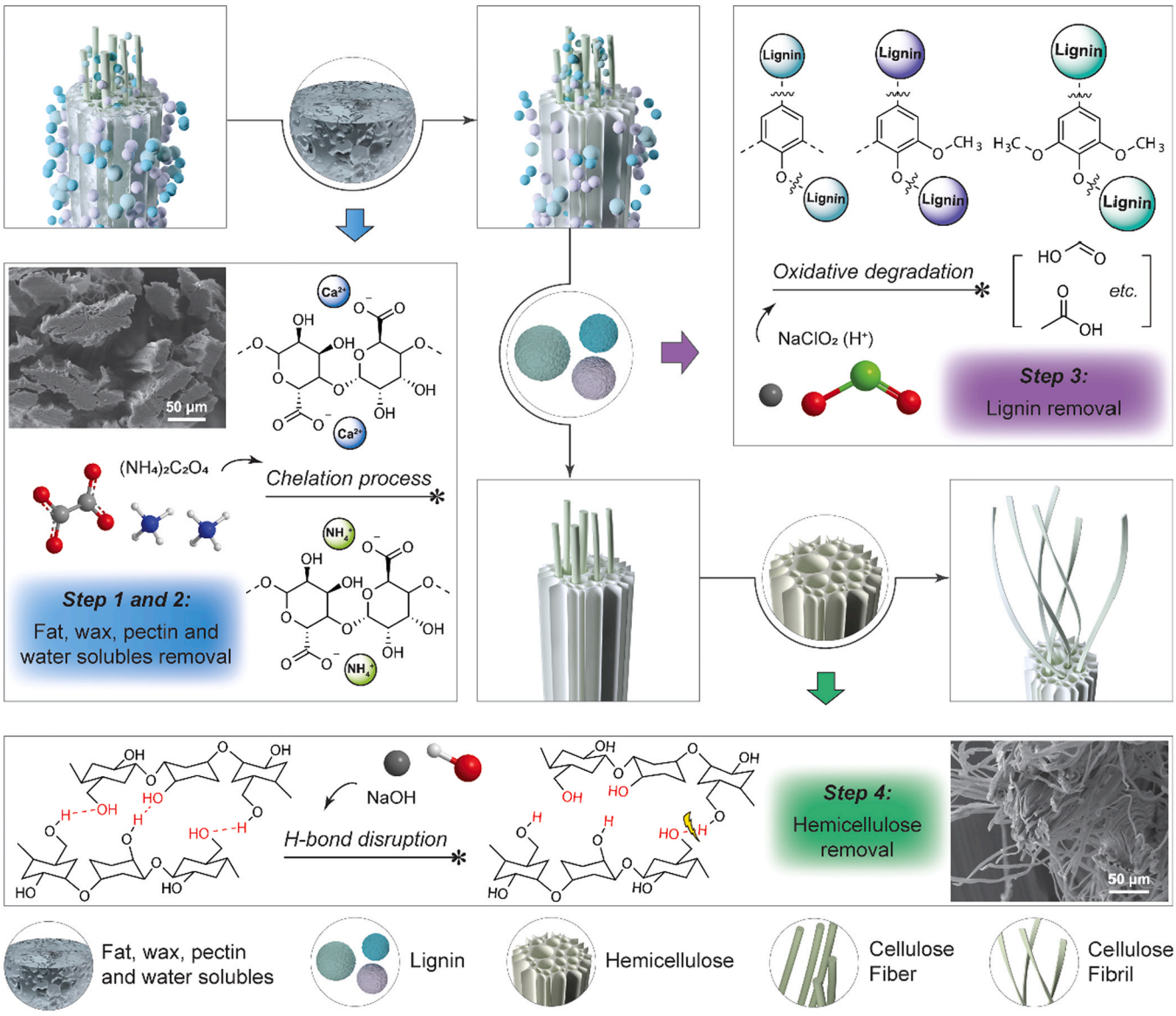

Fig. 1. Schematic of step-by-step degumming mechanism.

other cations. Typically, pectin contains metal ions such as calcium (Ca^{+}), which form cross-links with the carboxyl groups, stabilizing the pectin structure. $(NH_4)_2C_2O_4$ can chelate these metal ions, forming water-soluble complexes and disrupting the cross-linked structure of pectin (Thakur et al., 1997). This allows for the selective removal of pectin from fibers, enhancing the efficiency of the degumming process.

Step 3 focused on delignification by using sodium chlorite ($NaClO_2$), which transformed the appearance of PALF from light yellow to white. The reaction of $NaClO_2$ delignification in an acidic aqueous medium is given below:

$$NaClO_2 + H_2O \rightarrow HClO_2^-$$

$$5\ ClO_2^- + 2\ H^+ \rightarrow 4\ ClO_2 + Cl^- + 2\ OH^-$$

$$3\ ClO_2^- \rightarrow 2\ ClO_3^- + Cl^-$$

In this process, hypochlorous acid ($HClO_2$), chlorine dioxide (ClO_2), sodium chlorate ($NaClO_3$), and sodium chloride (NaCl) are generated. Chlorine dioxide (ClO_2) is considered the active compound, while chlorate (ClO_3^-) and chloride (Cl^-) ions are byproducts (Choudhury, 2006, 2011). ClO_2 acts as an oxidizing agent that targets phenolic hydroxyl groups and other easily oxidized functional groups in lignin. This process breaks down lignin into small, water-soluble molecules, facilitating its effective removal from PALFs (Liu et al., 2020).

In the final step, alkali treatment was used to remove hemicellulose from PALF. Hemicellulose consists of polysaccharide chains held together by hydrogen bonds. NaOH dissociates in water to form hydroxide ions (-OH), which effectively disrupt these hydrogen bonds. This disruption loosens the structure of hemicellulose, making it more soluble in alkaline solutions (Li et al., 2019). The -OH in hemicellulose can partially ionize under alkaline conditions, forming alkoxide ions. This ionization increases the hydrophilicity of hemicellulose, enhancing its interaction with water molecules and improving its solubility. Additionally, hemicellulose typically contains acetyl groups ($-COCH_3$), which are easily hydrolyzed under alkaline conditions to form acetate ions and free hydroxyl groups. This deacetylation not only enhances solubility but also reduces intermolecular cross-linking (Sjostrom, 2013). Consequently, alkali treatment effectively removes hemicellulose from PALFs.

As a result of the entire stepwise degumming process, SSD-PALF yielded a single pure component of cellulose fibrils. Intriguingly, the precise degumming method is capable of flexibly tuning the content of lignin and/ or hemicellulose residues within PALF for specific applications. Therefore, the fiber fineness can be regulated depending on the

PALF's compositions.

Step 1: Fat, Wax and Water-soluble Matter Removal

To remove impurities attached to fiber surface, all four types of raw PALF were subjected to an 8-h acetone treatment using a Soxhlet extractor to remove the fat and wax. This process was conducted at around 110 °C with a bath ratio of 1 g/20 mL. If the extract solution is still yellow after 8 h, the extraction will be extended until the solution becomes transparent. Following this treatment, the PALF samples were transferred to Erlenmeyer flasks containing distilled water.

To enhance solvent-gum interaction in the subsequent reaction, a spherical condenser was attached to each Erlenmeyer flask, and the mixtures were refluxed for 3 h to remove water-soluble components from PALF. The samples were then rinsed using a sieve and oven-dried at 50 °C. During the extraction process, the reaction solution was replaced once turning dark yellow.

Step 2: Pectin Removal

After removing fat, wax, and water-soluble matter, the pretreated PALF samples were placed into Erlenmeyer flasks containing 150 mL of 5 g/L $(NH_4)_2C_2O_4$ solution. Spherical condensers were attached, and the mixtures were boiled for 3 h. Subsequently, the fibers were rinsed using a sieve and dried in an oven at 50 °C.

Steps 3 and 4: Lignin and Hemicellulose Removal

For lignin removal, samples were immersed in a 3 % $NaClO_2$ solution at 80 °C for durations ranging from 1 to 8 h. The solution pH was adjusted to 4.6 using the CH_3COOH. For hemicellulose removal, samples were immersed in a 20 g/L NaOH solution at 105°C for durations of 4, 8, 12, and 16 h using a condensation reflux apparatus.

For the above two treatments, each gram of PALF was treated with 50 mL of the proposed solution. After treatment, samples were rinsed with deionized water to remove residual chemicals and dried. Characterization was repeated at least three times for each sample (5 g).

2.2.2. Lignin and Hemicellulose Quantification

Lignin and hemicellulose quantifications were performed according to the *GB 5889–86 Method of Quantitative Analysis of Ramie Chemical Components* with modifications, which is fundamental for regulating the gum content in PALF. The general procedures were as follows:

1) 3 g samples were first dried overnight at 80 °C to remove moisture, cooled to room temperature in a desiccator and weighed (G_0 for lignin, G_0' for hemicellulose).
2) For lignin: Samples were soaked in 30 mL of 72 % H_2SO_4 for 10 h, diluted to 300 mL with deionized water, and boiled for 4 h. For hemicellulose: Samples were boiled in a 20 g/L NaOH solution for 3 h.
3) Insoluble substances were separated using a vacuum filtration funnel. A Frit P40 type funnel (*ISO 4793*) was used. The dry mass of the filter (G_f) was recorded.
4) Samples were washed with deionized water to remove residual chemicals. For lignin quantification, the filtered residue was washed until the filtrate was free of sulfate ions, indicated by the absence of precipitate when 10 % $BaCl_2$ solution was added. For hemicellulose quantification, the filtered residue was washed until the filtrate reached a pH of 7.
5) The resultant filter or fibers were dried at 105 ± 3 °C in a ventilated oven until a constant mass was achieved.
6) After cooling to the room temperature in a desiccator, the final masses were recorded (G_1 for lignin, G_1' for hemicellulose).

The relative content of each component was calculated using Eqs. (1) and (2):

$$W_{lignin} = \frac{G_1 - G_f}{G_0} \times 100\% \quad (1)$$

$$W_{hemicellulose} = \frac{G_1' - G_0'}{G_0'} \times 100\% \quad (2)$$

Each sample was measured three times to get the average value.

2.2.3. Surface morphology and structure

Scanning electron microscope (Tescan VEGA3) was employed to examine both the cross-sectional and longitudinal surface morphology of the fiber samples. To observe the cross-sectional structure, the fiber bundles were first soaked in ethanol for 10 h, followed by overnight drying in an oven at 60 °C to remove moisture. The dried bundles were then immersed in liquid nitrogen for 3 minutes. Immediately upon removal from the liquid nitrogen, the fiber samples were cut by a sharp blade to show a smooth and complete cross section.

2.2.4. FTIR test

Fourier transform infrared spectroscopy (FTIR, PerkinElmer Inc., USA) was used to further indicate the component change in fibers during degumming. Changes in chemical component can be indicated by shifts in frequency, variations in peak intensities, and alterations in the FTIR spectral shape, which validate the morphology change (Fig. 2) and quantitative analysis of PALF at different degumming stages (Fig. 5).

2.2.5. Width measurement

The fibrils were observed and imaged using an optical microscope (M165C, Leica, Switzerland). The open-source package Diameter J plug-in was employed to measure fibril width by analyzing the captured images. Data were collected from 200,000 measurements across 1000 fibrils in each sample group.

2.2.6. Antibacterial test

The natural antibacterial performance of PALF was evaluated using the shake flask test, as outlined in *GB/T 20944. 3–2008 Textiles-Evaluation for antibacterial activity-Part 3: Shake Flask Method*. The bacteria strains used in the test included *Escherichia coli (ATCC 8099)*, *Staphylococcus aureus (ATCC 6538),* and *Candida albicans (ATCC 10231)*. Each sample of 10 g was prepared, with 100% cotton fabrics (standard adjacent fabric) taken as the control group. After sterilization via high-pressure steam, the samples were placed in flasks containing the bacterial solution and cultured for 18 h under controlled conditions. The bacterial concentration in the culture solution was then measured, and the antibacterial rate was calculated using Eq. (3):

$$Y = \frac{W_t - Q_t}{W_t} \times 100\% \quad (3)$$

where Y is the bacteriostatic rate (%), W_t is the average bacterial concentration (CFU/mL) for the control sample and Q_t is the average bacterial concentration for the test sample.

2.2.7. Thermogravimetric analysis

The thermal decomposition of raw and degummed PALF was evaluated by a thermogravimetric analysis (TGA 4000, PerkinElmer Inc., USA). Samples weighing 5 mg were placed in a platinum pan, and tests were carried out in a programmed temperature range of 30 – 800 °C at a heating rate of 20 °C/min under a nitrogen atmosphere at a flow rate of 19.6 mL/min.

3. Results and discussion

3.1. Morphology and structure of PALF

As shown in Fig. 2a, four varieties of raw PALFs (45–75 μm in width) exhibited varying degrees of yellowness and brightness, ranging from dark to light yellow. These variations can be explained by several factors, such as pineapple variety, growth environment, extraction method,

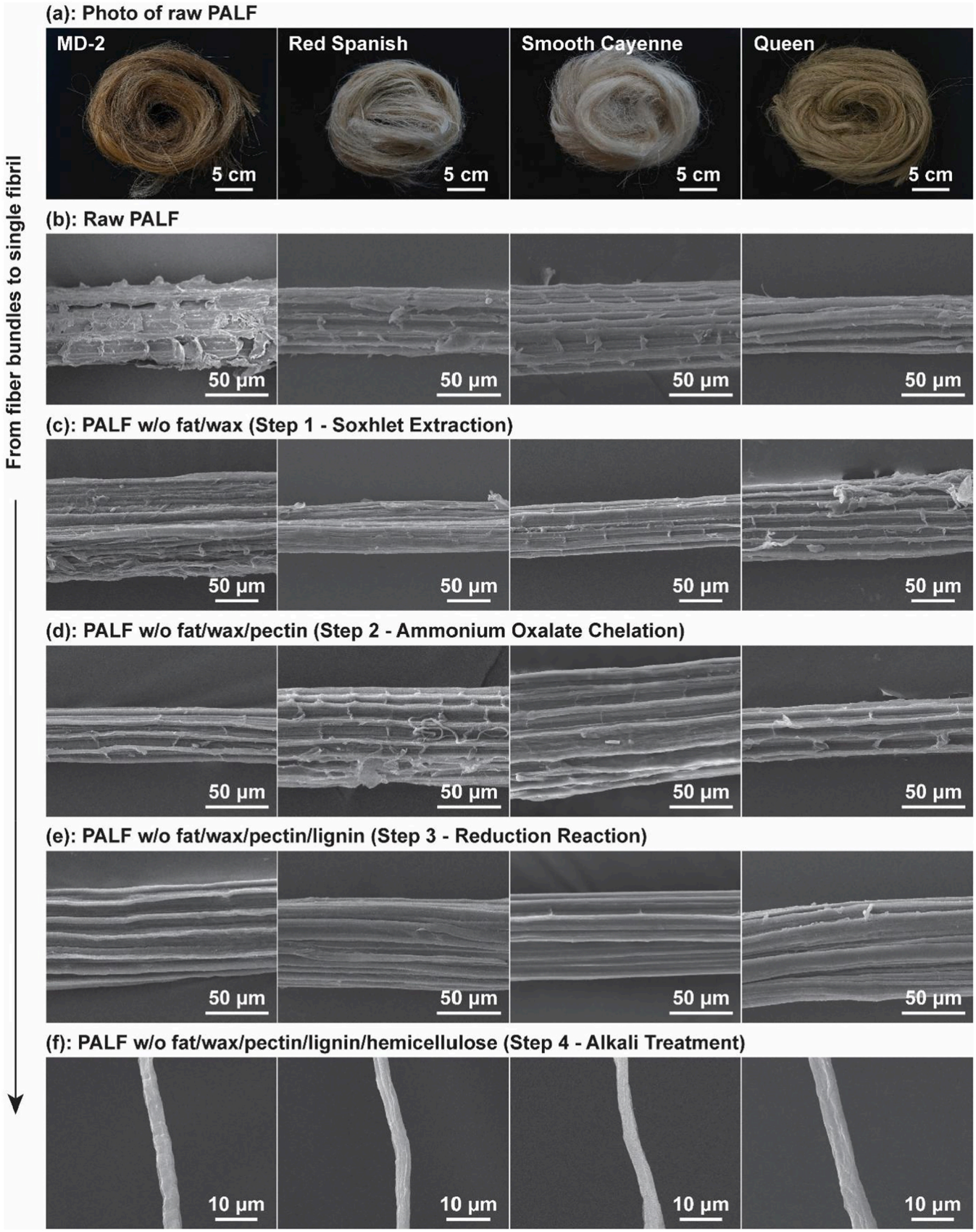

Fig. 2. Longitudinal morphology of four kinds of PALF. (a) Raw PALF photograph; (b-f) SEM images showing the morphology change of fiber's longitudinal surface during SSD. (b) Raw PALF; (c) PALF after removal of fat, wax, and water-soluble matter through Soxhlet Extraction (step 1 in SSD); (d) After removal of pectin through ammonium oxalate chelation (step 2), PALF composed of lignin, hemicellulose, and cellulose; (e) After delignification through reduction reaction (step 3), PALF composed of hemicellulose and cellulose; (f) After removal of hemicellulose through alkali treatment (step 4), pineapple leaf fibril composed of solely cellulose.

post-extraction drying temperatures, and storage conditions. All raw PALF bundles displayed substantial gum with visible transverse nodes and longitudinal grooves on the outer layer. The rough surface was covered with scaly fat and wax (Fig. 2b). During the degumming process, each component was specifically and precisely removed, resulting in morphological changes primarily in color, width, length, and surface roughness. In the first step, as shown in Fig. 2c, the fiber surfaces became smoother after removal of fat and wax through Soxhlet extraction method using acetone. The fat and wax served as the protective coating layer on the fiber surface, which makes it more hydrophilic and susceptible to the following chemical treatments after step 1. In step 2, although the pectin was removed by ammonium oxalate chelation, transverse nodes could be still observed (Fig. 2d). Interestingly, from the viewpoint of cross section (Fig. 3a and b), the original tightly packed fiber bundles became loose with minor gaps (< 1 μm) after sequential removal of fat, wax and pectin.

In step 3, PALF treated with $NaClO_2$ for lignin removal showed a remarkable change in surface structure, where transverse nodes were thoroughly removed with prominent longitudinal ravines (Fig. 2e). In the absence of lignin, the gaps between fibers widened, although individual fibers remained encapsulated by adhesive gum, maintaining the bundle structure (Fig. 3c). This occurs because lignin exists as small particles attached to the longitudinal section of the fiber (Österberg et al., 2020), while hemicellulose occupies spaces between the fibrils, binding them together like annular ties (Wan et al., 2010). Finally in step 4, removal of hemicellulose caused PALF bundles to separate into short, thin fibrils with clear, smooth and ribbon-like structure (Fig. 2f and Fig. 3d). From step 3–4, individual fibril can be obtained with much smaller width than the original fiber bundles. Therefore, it is concluded that hemicellulose is the key component to control PALF fineness.

3.2. The fineness of fibrils

Understanding individual fiber fineness is essential for determining how many single fibers need to be bonded together to meet spinning requirements for both fiber fineness and length. This knowledge can help optimize the degumming process to achieve the desired fiber properties. Fig. 4 shows the width distribution of fibrils across four PALF varieties. The DiameterJ plugin software was used to analyze and calculate the fibril width across all examined PALF varieties through Gaussian fitting. This analysis revealed the fibril width: 5.5 ± 0.4 μm for MD-2; 4.1 ± 0.4 μm for Red Spanish; 5.3 ± 0.5 μm for Smooth Cayenne and 4.5 ± 0.5 μm for Queen. Basically, the fibril width falls within 4.1–5.5 μm for these four varieties, which is comparable to the minimum fineness of jute fibers (5 μm) (Franck, 2005). This result suggests that all these varieties have potential for fine fiber production. Notably, all PALF varieties exhibited finer fibril than single cotton fiber (12–22 μm in width) (Liu et al., 2022). From the fitting curves, the full width at half maximum (FWHM) of Red Spanish PALF is the lowest, indicating the narrow distribution of width. This characteristic suggests more uniform fibril fineness in Red Spanish than in other varieties examined in this study.

3.3. Quantitative analysis of PALF components

The chemical composition of four types of PALF was quantitatively analyzed using the weight loss method following the *GB 5889–86* standard. Table 1 shows the detailed composition ratios of PALF with notable variation among varieties, which is consistent with the results in previous literature (Fareez et al., 2018; Mishra et al., 2004; Neto et al., 2015). The composition of fat, wax, water-soluble materials, and pectin varied greatly among the four varieties. By contrast, lignin content showed minimal variation across the varieties (~ 5 %), with an average of approximately 0.15 g per 3 g sample. Queen PALF contained the highest proportion of lignin at 6.6 %, which may contribute to enhanced fiber modulus (Jakob et al., 2022) and potential antibacterial properties (Ali et al., 2024). Smooth Cayenne and Queen PALF exhibited higher cellulose content (>60 %). This suggests great potential for them to obtain better mechanical properties, as cellulose is the primary contributor to fiber strength and stiffness (Jakob et al., 2022).

MD-2 PALF demonstrated the highest weight loss in acetone and boiling water, indicating elevated levels of fat, wax, and water-soluble

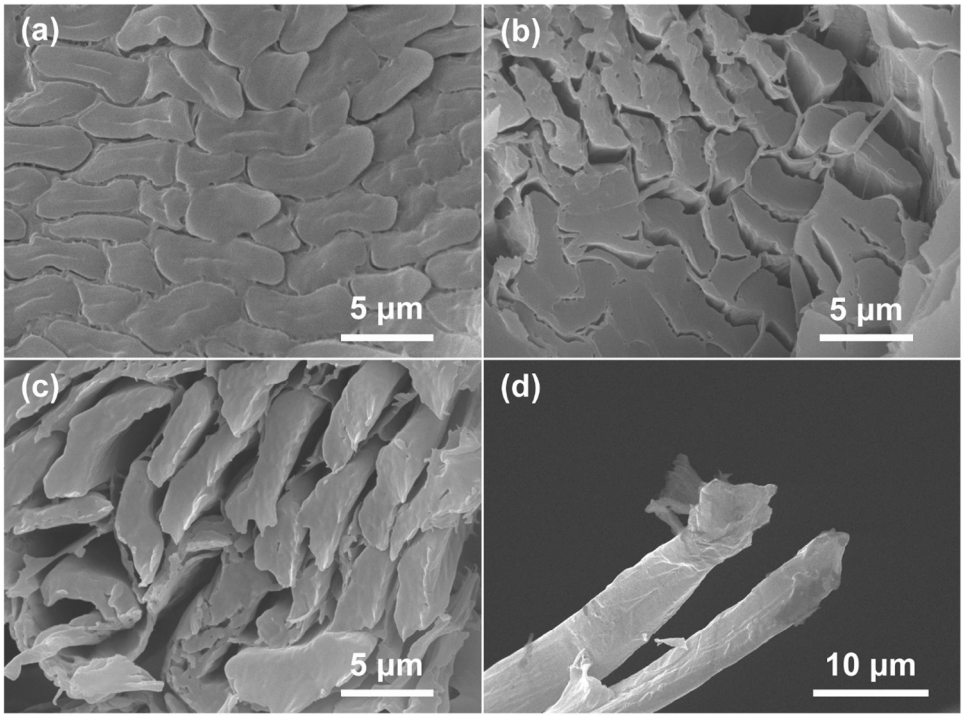

Fig. 3. Cross-sectional structure of Queen PALF during SSD. (a) Raw PALF; (b) PALF after degumming step 2, composed of lignin, hemicellulose and cellulose; (c) PALF after degumming step 3, composed of hemicellulose and cellulose; (d) Pineapple leaf fibrils after degumming step 4, composed of cellulose.

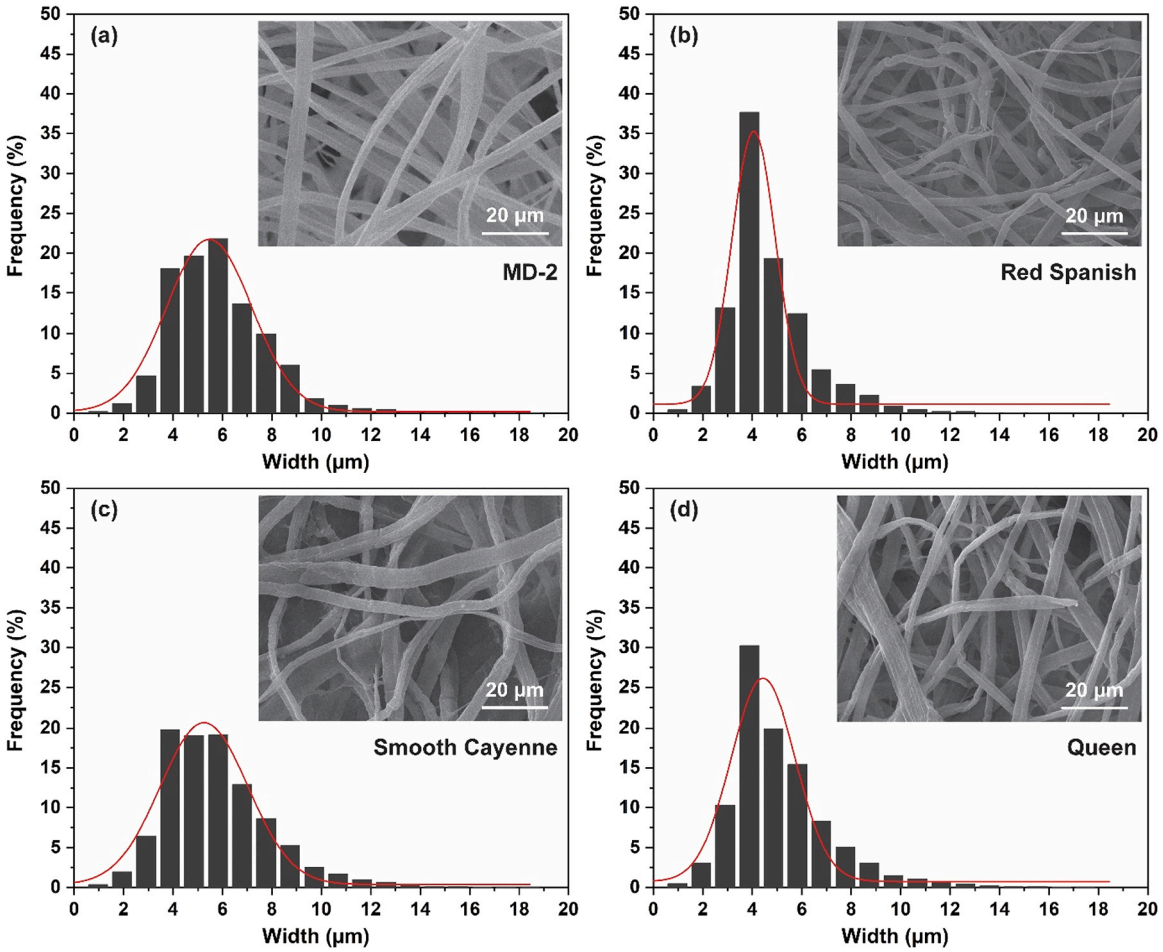

Fig. 4. Fibrils width distribution across four PALF varieties. (a) MD-2 PALF;(b) Red Spanish PALF; (c) Smooth Cayenne PALF;(d) Queen PALF. Inset images: Representative SEM images of fibrils from each variety. Red line: Gaussian fitting curve. Data based on 200,000 measurements across ~1000 fibrils per sample group.

Table 1
Chemical composition of PALF from four different varieties.

Category	Fat and Wax	Water Soluble Materials	Pectin	Lignin	Hemicellulose	Cellulose
MD−2	4.3 ± 0.6 %	9.5 ± 2 %	16.7 ± 3.2 %	4.6 ± 1.6 %	34. 5 ± 8.9 %	30.4 ± 11.0 %
Red Spanish	1.9 ± 0.2 %	5.4 ± 1.7 %	2.0 ± 0.3 %	4.5 ± 0.7 %	38.0 ± 1.1 %	48.3 ± 9.2 %
Smooth Cayenne	0.1 ± 0.1 %	2.3 ± 0.1 %	0.9 ± 0.4 %	5.8 ± 0.9 %	28.2 ± 1.2 %	62.7 ± 3.9 %
Queen	1.3 ± 0.5 %	0.2 ± 0.1 %	8.0 ± 1.1 %	6.6 ± 0.3 %	22.1 ± 0.9 %	61.9 ± 4.1 %

pigments (~ 13.8 %). These extracts may increase chemical consumption and processing time during degumming. Conversely, Queen PALF contained only 1.5 % of these purities, potentially simplifying the degumming process. Furthermore, Queen pineapple is the predominant variety in China, occupying more than 70 % of the pineapple cultivation area (Liu et al., 2024). This prevalence presents a principal advantage for potential industrial scale-up and sustainable sourcing. Queen PALF emerged as the most promising variety for industrial applications due to its favorable composition: high cellulose content (> 60 %), high lignin content (6.6 %), and low soluble impurities (1.5 %). Therefore, Queen PALF was selected for precise degumming to obtain specific components in the following section.

Fig. 5 illustrates the chemical composition of Queen PALF at each stage of the stepwise degumming process. The samples are categorized as follows: Raw PALF, S1 (PALF after step1 to remove fat and wax), S2 (PALF after steps 1 and 2 to remove fat, wax, and pectin), S3 (PALF after steps 1–3, which removes fat, wax, pectin, and lignin), and S4 (PALF after all four degumming steps). As shown in the figure, the SSD-PALF effectively removed specific gum component without significantly affecting others. The cellulose content steadily increased, reaching nearly 100 % in S4, indicating the successful separation of fibrils after the completion of all four degumming steps. The progressive removal of lignin and hemicellulose is detailed in Section 3.5, where the detailed variations in their content are discussed with different treatment times.

3.4. FTIR analysis of SSD-PALF

FTIR was used to investigate changes in chemical bonds and confirm the removal of lignin, hemicellulose, and other residual gums, the infrared spectra were shown in Fig. 6. The characteristic COO^- stretching bond for pectin appears at 1456 cm^{-1} (Célino et al., 2013) in raw PALF and S1 but disappears in the subsequent samples, indicating a thorough removal of pectin after steps 1 and 2. The C═C stretching bond that come from aromatic compounds at 1509 cm^{-1} characteristic of lignin, disappears in S3 and S4, indicating lignin removal. Additionally, the CH_3 stretching at 2954 cm^{-1}, originating from aromatic compounds in lignin, becomes very faint in samples S3 and S4, further confirming that there is almost no lignin remaining in these samples. The vibrational

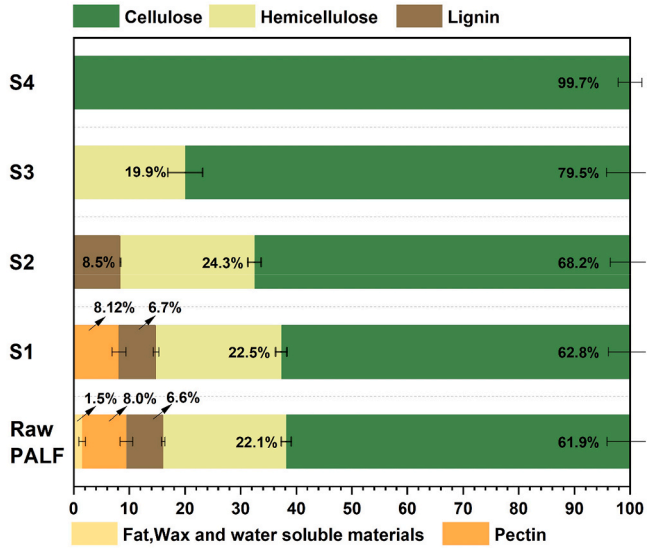

Fig. 5. Chemical composition of Queen PALF at different degumming stages.

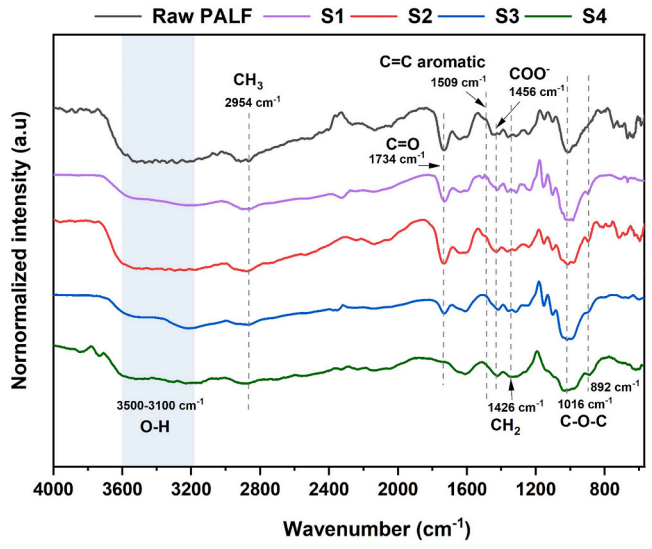

Fig. 6. The FTIR spectrum of Queen PALF at different degumming stages.

mode for hemicellulose, observed at 1734 cm^{-1} due to C═O stretching disappears after step 4 (Grumo et al., 2017), confirming hemicellulose removal. The range between 3500 and 3100 cm^{-1}, representing –OH stretching vibrations, becomes more pronounced in S4, reflecting increased exposure of hydroxyl groups as all gum residues have been removed and cellulose becomes more detectable. The characteristic cellulose vibrational modes are found at 1426 cm^{-1} (CH_2 symmetric bending), 1016 cm^{-1}, and 892 cm^{-1} (asymmetric C-O-C bridge stretching and anhydroglucose ring asymmetric stretching) (Célino et al., 2013).

The changes in the FTIR spectra correlate with the results obtained in quantitative analysis of fiber composition (Fig. 5), demonstrating the selective and efficient removal of the non-cellulosic components and confirming the progressive purification of PALF during the step-by-step degumming process.

3.5. *Flexible regulation of lignin and hemicellulose residues*

To better understand the reduction trends of hemicellulose without the influence of other gums and to maximize the removal of hemicellulose residues, lignin was first extracted in step 3, followed by the removal of hemicellulose in step 4 during the fibril separation process. The residual contents across all four PALF varieties were recorded over time (Figs. 7a and 7c). As the tendency for the lignin and hemicellulose residue as a function of time was similar for all PALF varieties, the profiles were combined in Fig. 7b/ 7d to show the overall change of residues with the treatment time. Apparently, there exist two stages for both residues. In the first stage, a sharp decline of lignin and hemicellulose residues was observed in the first 3 h; then in the second stage, it became more stable for the change of residue in the following 5 h. As shown in Fig. 7b, the lignin residue can be predicted by the linear fitting result with high values of R^2 (> 0.9). Initially, lignin decreased rapidly at a rate of approximately 1 % per hour, which can be attributed to the removal of lignin located in the lamella near the fiber surface. Subsequently, it shifted to the lignin situated in the cell wall inside the fiber (Lee et al., 2020). After 8 h of treatment, the lignin residue approached

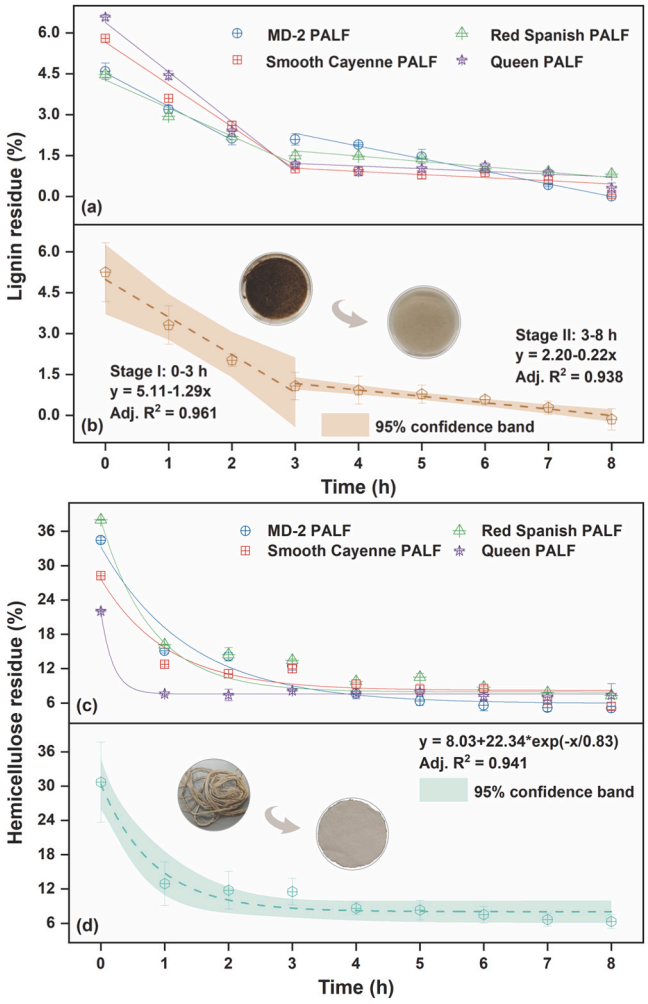

Fig. 7. Gum residues over time across four PALF varieties during SSD. (a) Four lines illustrate the line fitting results of the lignin residue of each PALF variety over time during delignification (step 3). (b) The brown fitted line represents the average lignin residue of four PALF varieties over time during step 3, which could be divided into two stages. Stage I is fitted with the line of $y = 5.11 - 1.29x$; Stage II is fitted with the line of $y = 2.20 - 0.22x$; with inset images showing the extracted lignin from samples treated for 0 and 8 h (step 3). (c) Four fitted curves illustrate the hemicellulose residue over time for each PALF variety. (d) The Green fitted curve represents the average hemicellulose residue over time during hemicellulose removal (step 4), fitted with $y = 8.03 - 22.34e^{-\frac{x}{0.83}}$, with inset images showing PALF treated by alkali treatment for 0 and 8 hours (step 4).

~0 %, indicating that almost all lignin had been extracted from the PALF in the funnel.

In the case of hemicellulose (Fig. 7d), a rapid decrease was observed within the first 1 h, in which more than half of the hemicellulose could be removed. In the next two hours, the PALF bundles gradually split into individual fibrils accompanied by a slight decrease in hemicellulose residue. Interestingly, when the treatment time was increased from 4 to 8 h, the hemicellulose residue was stable and maintained around 7.5 %. Complete elimination of hemicellulose could not be achieved by extending the treatment duration, as a portion of hemicellulosic fractions were tightly entangled with cellulose. This structural feature impedes the stretching and interruption of molecular chains by hydroxyl groups (Li et al., 2019). Therefore, a treatment duration of 4 h in step 4 appears to be most effective for hemicellulose removal. Further extension of the treatment time could potentially damage cellulose with resultant low crystallinity and degree of polymerization, thereby compromising fiber quality and hindering accurate quantification of gum content.

To achieve low hemicellulose but high lignin ratio in PALF, it is feasible to reverse the degumming sequence in step 3 and step 4. Fig. 8 presents hemicellulose and lignin residues in Queen PALF over time after reversing the degumming sequence. By using alkaline solution, the hemicellulose content in PALF seriously decreased, finally stabilizing at around 3 % after two hours of treatment. Concurrently, the relative lignin ratio reached a maximum of 12.8 %, nearly double the original value. As the reaction progressed, the hemicellulose content stabilized, and the fiber weight no longer decreased significantly. Additionally, some lignin could be lost during alkaline treatment. From the fitting results, it is concluded that the highest lignin ratio in PALF could be achieved by conducting a 1.5–2 h treatment of hemicellulose residues. In summary, it is flexible to control relative ratios of hemicellulose and lignin within PALF with the SSD method. This will allow a suitable relative ratio of each component to be obtained to achieve balanced properties of PALF in terms of antibacterial performance, mechanical properties, and fineness.

3.6. Control of fiber fineness via hemicellulose residues

As mentioned in morphology characteristics of PALF, hemicellulose content influences fiber fineness greatly. Based on the fitted curve in Fig. 8, various hemicellulose residue ratios can be obtained under distinct treatment time from 0 h (H_0), 0.5 h ($H_{0.5}$), 1 h (H_1) to 1.5 h ($H_{1.5}$). Correspondingly, the calculated hemicellulose residue ratios were 23.5 %, 9.4 %, 5.9 %, and 4.9 %, respectively.

Fig. 9 illustrates the relationship between fiber fineness and the hemicellulose residue ratio, which ranges from 4% to 24 %. The mean fineness of sample H_0 was 60.2 ± 30.7 μm, thicker than ramie fibers (40 ± 24 μm, shown in Table 2) (Franck, 2005). After 0.5 h of alkaline treatment ($H_{0.5}$), approximately half of the hemicellulose was removed, resulting in a pronounced reduction of more than 50 % in fiber width. The average fineness of $H_{0.5}$ was 25.5 ± 7.3 μm, comparable to flax fibers (19 ± 10 μm, shown in Table 2) (Franck, 2005). While some fibers as thin as 10 μm were observed, the majority of the fiber bundles remained intact, with around 6.5 % of the fibers being separated. Further treatment (H_1 and $H_{1.5}$) resulted in even smaller fibers, with the average fineness decreasing to to 18.6 ± 6.0 μm for H_1 and 16.7 ± 5.0 μm for $H_{1.5}$. This trend is reflected in the shift of the fiber width distribution peak to the left, indicating an increased proportion of individual fibers, with the highest frequency reaching 10 %. Additionally, the *SD* of fiber width decreased progressively from 30.7 μm in H_0 to 5.0 μm in $H_{1.5}$. This indicates that as hemicellulose content decreased, the fiber fineness became more uniform. The uniformity of the degummed PALF fibers with varying treatment durations is clearly visible in the SEM images shown in Fig. 7.

These results reveal a strong relationship between hemicellulose ratio and fiber fineness, which is mainly attributed to hemicellulose's role in binding cellulose and its contribution to the overall fiber structure (Wan et al., 2010). In PALF bundles, the ultimate fibrils, composed solely of cellulose, are arranged in a spiral pattern, while hemicellulose, lignin, and other residual gums (pectin, fat, and wax) are distributed randomly, creating a complex matrix. Notably, the hemicellulose content (~22.1 %) plays a crucial role in maintaining the integrity of the fiber matrix, while lignin constitutes only 6.6 %, suggesting that it is the hemicellulose that primarily supports the matrix. Removal of lignin does not significantly destabilize the matrix, whereas the removal of hemicellulose through alkali treatment disrupts not only the hydrogen bonds within the hemicellulose but also those between hemicellulose and cellulose. This weakening of cohesion between fibrils facilitates the separation of fiber bundles into finer individual fibers. Surpporting theses findings, the achieved fiber fineness of samples $H_{0.5}$, H_1, and $H_{1.5}$ (25.5, 18.6, and 16.7 μm, respectively) approaches the typical fiber

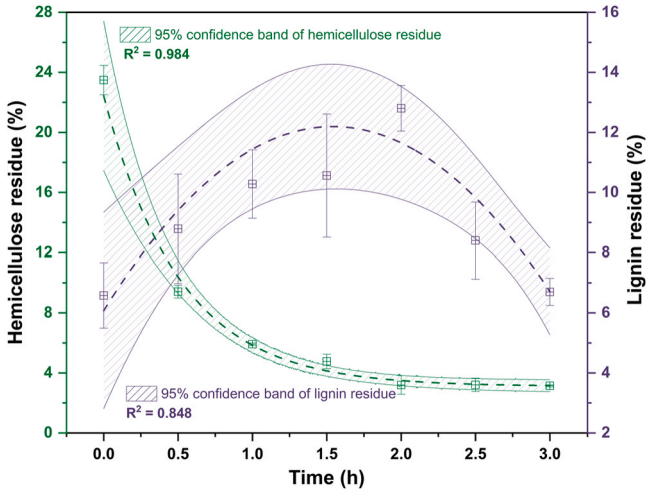

Fig. 8. Hemicellulose and lignin residue in Queen PALF by reverse SSD degumming. The green fitted curve displays hemicellulose residue over time with 95 % of confidence band: $y = 3.10 - 20.35e^{-\frac{x + 0.03}{0.51}}$, with high correlation coefficient of 0.984. The purple fitted curve displays lignin residue over time with 95 % of confidence band: $y = 6.08 + 7.94x - 2.57x^2$, with a correlation coefficient of 0.848.

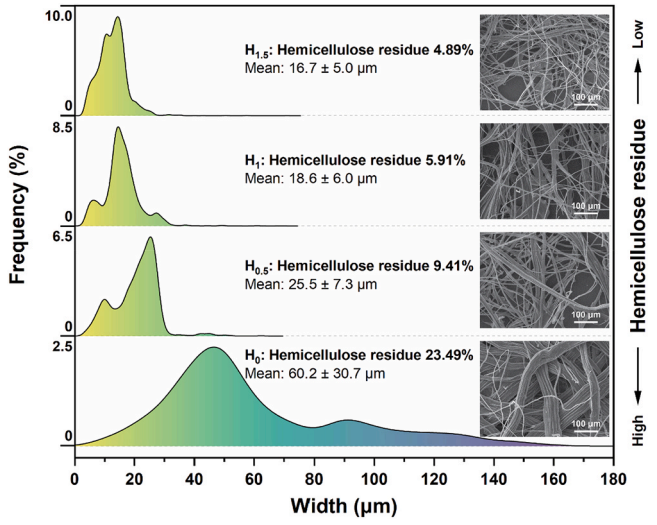

Fig. 9. Fiber fineness of Queen PALF at various hemicellulose residue ratios under reverse SSD degumming. Inset images: Representative SEM images for each PALF sample. Data (Mean ± *SD*) based on 3000 measurements from 10 images per group, are statistically calculated as frequency (probability).

Table 2
Fineness, bacteriostatic rate, and thermal stability of various bast fibers.

Nature Fiber	Fineness (μm)	Bacteriostatic Rate (%)	Onset oxidation temperature (℃)	Ref
Jute	5–25	99.1 % against *E. coli* 48 % against *S. aureus*	170	(Xi et al., 2013) (Ivanovska et al., 2020)
Flax	19 ± 10	46.62 % against *E. coli* 8.7 % against *S. aureus*	170	(Tian et al., 2016)
Kenaf	50–70	~ 89 % against *E. coli* ~ 86 % against *S. aureus*	260	(Ramesh, 2016) (Zakaria et al., 2011)
Ramie	40 ± 24	81.29 % against *E. coli* 90.2 % against *S. aureus*	200–300	(Wei et al., 2023)
Sisal	50–200	Not against *E. coli* and *S. aureus*	200	(Trivedi and Gupta, 2023)
Bagasse	10–34	Not against *E. coli* and *S. aureus*	207	(Abdelwahab and Shukry, 2015)
Bamboo	25–40	3–50 % against *S. aureus* Not against *E. coli*	/	(Prang Rocky and Thompson, 2021)
Raw Queen PALF	45–75	94.8 % against *E. coli* 98.2 % against *S. aureus* 90.3 % against *C. albicans*	304	Our work
Degummed Queen PALF	16.7 ± 5	94.6 % against *E. coli* 98.4 % against *S. aureus* 89.6 % against *C. albicans*	339	Our work

fineness of cotton fibers (12–22 μm) (Liu et al., 2022).This suggested that these degummed PALF could potentially be processed using existing cotton spinning systems, provided that the length of degummed PALF is also suitable.

3.7. Thermal stability

To evaluate the thermal stability of PALF after stepwise degumming, thermogravimetric analysis (TGA) was conducted on raw Queen PALF) and a series of degummed Queen PALF (S1, S2, S3, $H_{1.5}$). As illustrated in Fig. 10, an initial weight loss occurred around 100 °C due to the evaporation of bound water molecules within the fibers. Between 270 °C and 410 °C, all PALF samples exhibited significant weight reduction, corresponding to the thermal degradation of major fiber components, including cellulose, hemicellulose, lignin, and pectin.

The onset decomposition temperatures for raw and the finest degummed fibers ($H_{1.5}$) were respectively determined to be 304°C and 339°C, exceeding those documented for other bast fibers (Table 2). It indicates that raw PALF decomposes at a lower temperature and the increase in onset decomposition temperature is primarily due to the removal of small molecular-weight components such as waxes, pectin, and other water-soluble materials during the degumming process. At 700 °C, the raw PALF retained approximately 0.54 % residue, while degummed samples exhibited higher residual masses. Specifically, samples S3 and $H_{1.5}$ showed the highest residual content, around 15.56 %. This is attributed to the release of large amounts of combustible gases from fat, wax and lignin during combustion, which promote

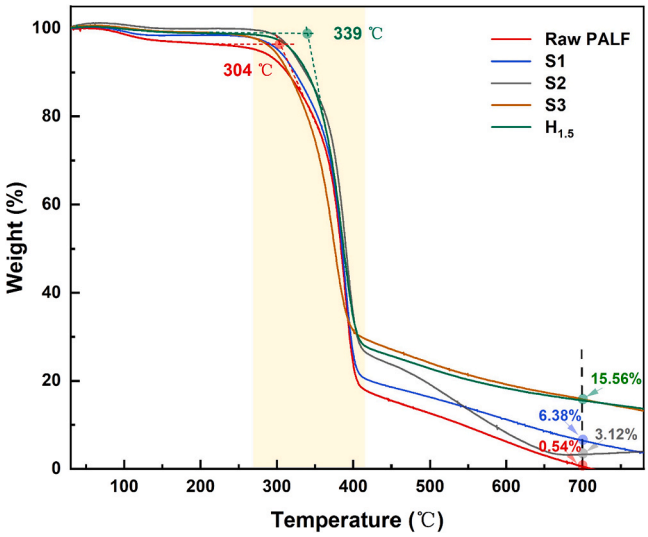

Fig. 10. TGA curves of raw and degummed Queen PALF.

burning (Grumo et al., 2017). Conversely, pectin tends to form a char layer that inhibits combustion, explaining why S1, which still contains pectin, showed greater residue than S2.

Overall, the SSD method enhances the thermal stability of PALF by removing easily degradable components, making degummed PALF more suitable for applications requiring exposure to high temperatures (above 300°C), such as in the automotive, aerospace, or construction industries (Reddy et al., 2020). However, for environments exceeding 350–400°C, additional treatments or the incorporation of suitable composite matrices may still be necessary.

3.8. Antibacterial properties

The study compared the antibacterial effectiveness of the finest degummed PALF ($H_{1.5}$) with that of raw PALF against three bacterial strains: *S. aureus*, *E. coli*, and *C. albicans*. The bacterial counts after an 18-h culture period and the corresponding bacteriostatic rates of $H_{1.5}$, raw PALF, and a negative control group (Control fabric 100 % cotton) were determined using Eq. (3).

As shown in Table 3, both raw and degummed PALF exhibited strong antibacterial properties according to the *GB/T 20944.3–2008* standard. Their bacteriostatic rates exceeded the required thresholds of antibacterial efficacy, namely > 70 % for *S. aureus* and *E. coli*, and > 60 % for *C. albicans*. More specifically, the results indicated that both degummed and raw PALF exhibited robust bacteriostatic rates against *S. aureus* and *E. coli*, exceeding 98 % and 94 %, respectively. This result suggests no significant difference in antibacterial properties between both samples for these bacteria. Furthermore, these bacteriostatic rates are notably higher than those of other bast fibers. For instance, the bacteriostatic rate of ramie against *S. aureus* is 90.2 % (shown in Table 2), while jute and flax fibers exhibit rates of 48 % and 8.7 %, respectively (Xi et al., 2013). The bacteriostatic rates of ramie and flax against *E. coli* are 81.29 % and 46.62 % (Table 2), respectively (Tian et al., 2016; Wei et al., 2023). Additionally, the bacteriostatic rate against *C. albicans* of both raw and degummed PALF was high (~ 90 %), surpassing that of other bast fibers as well (Li et al., 2012; Xi et al., 2013).

Interestingly, despite the difference in lignin content between $H_{1.5}$ (~ 10 %) and raw PALF (~ 6.8 %), no obvious variation in colony counts was observed, indicating the high potency of even a modest amount of lignin in achieving good antibacterial performance. It is also possible that other components in fibers, aside from polyphenol, such as terpenes, flavonoids, esters, and lactones (Zamora-Mendoza et al., 2022), may contribute to the observed antibacterial properties. The degumming method adopted in our work will help maintain the intrinsic

Table 3
Antibacterial properties of raw and degummed Queen PALF.

Sample Group	Bacteria Type	Total Bacterial Count (CFU/mL)			Growth Value F	Antibacterial Rate (%)
		Negative Control		PALF		
		Contact 0 h	After 18 h cultivation	After 18 h cultivation		
Raw Queen PALF	*S. aureus*	2.0×10^4	2.9×10^6	5.2×10^4	2.2	98.2
	E. coli	2.2×10^4	8.5×10^6	4.4×10^5	2.6	94.8
	C. albicans	1.9×10^4	6.8×10^5	6.6×10^4	1.6	90.3
Degummed Queen PALF ($H_{1.5}$)	*S. aureus*	2.0×10^4	2.9×10^6	4.5×10^4	2.2	98.4
	E. coli	2.2×10^4	8.5×10^6	4.6×10^5	2.6	94.6
	C. albicans	1.9×10^4	6.8×10^5	7.1×10^4	1.6	89.6

antibacterial performance, making it a promising material for the development of functional textiles with antimicrobial characteristics. For example, like other bast fibers, PALF's porous structure makes it particularly effective against anaerobic bacteria (Huang et al., 2014), positioning it as a potential candidate for applications in medical textiles, wound dressings, and antifungal materials. Moreover, when incorporated into biodegradable packaging, PALF may play a key role in enhancing food safety, offering a sustainable solution for the healthcare and packaging industries (Todhanakasem et al., 2022).

4. Conclusion and outlook

In this work, we developed a step-by-step degumming (SSD) method for pineapple leaf fibers (PALF) to flexibly control the component ratios of lignin and hemicellulose residues and fiber fineness from bundles to fibrils. The research encompassed multiple PALF varieties, including MD-2, Red Spanish, Smooth Cayenne, and Queen, with the latter emerging as the most promising for industrial applications due to its favorable composition and prevalence in cultivation.

The SSD method was designed to target specific components while minimizing damage to others, effectively transforming the morphology of PALF from tightly packed bundles to separated, ribbon-like fibrils. This process highlighted the crucial role of hemicellulose in maintaining fiber bundle integrity, with its removal recognized as the key factor influencing fiber fineness. The optimized degumming sequence not only reduced hemicellulose content but also managed lignin levels effectively, enhancing overall PALF quality. Remarkably, the study demonstrated that the SSD method could refine PALF to achieve fineness comparable to, or even finer than, cotton fibers, with mean fibril widths ranging from 4.1 to 5.5 μm across varieties. This result underscores the potential of PALF as a high-quality natural fiber for different applications. Most importantly, the research revealed that the proposed degumming method preserved the inherent antibacterial properties of PALF. Both raw and degummed PALF exhibited strong bacteriostatic activity against *S. aureus*, *E. coli*, and *C. albicans*, with rates exceeding industry standards.

Building on these findings, future efforts on PALF refining should pursue several key directions to advance its practical application and fully exploit its potential as a sustainable, high-performance natural fiber:

1) The preservation of antibacterial properties alongside physical refinement opens new avenues for developing antimicrobial textiles from sustainable sources. Even a modest level of lignin content in degummed PALF has good antibacterial activity, which may be enhanced by the presence of other phenolic compounds. This observation highlights the need for further investigation into PALF's complex phytochemistry. It presents opportunities for optimizing both the physical and antibacterial properties of PALF-based products through targeted processing techniques.
2) Although improvements in fiber fineness have been achieved, the relationship between fiber dimensions and mechanical properties warrants further exploration. Future work should examine how varying fiber fineness affects tensile strength, durability, and elasticity, and distinguish the mechanical contributions of specific fiber components. These insights will inform the tuning of degumming and processing parameters to produce fibers with optimal mechanical properties suitable for spinning, nonwoven production, and other industrial applications.
3) Efficient waste management is essential, given that the degumming process produces "black liquor" containing lignin derivatives, hemicellulose, and other organic compounds. Techniques such as distillation, condensation, membrane separation, and crystallization can recover and concentrate valuable reagents. For instance, wasted acetone can be evaporated, condensed, and returned to the next Soxhlet extraction cycle for a closed-loop recycling, lowering reagent costs and mitigating the environmental impact. By employing these recycling strategies and exploring alternative green chemicals, the degumming process can be made more sustainable and cost-effective.
4) Currently, the entire stepwise degumming process exceeds 14 h. To address this, integrating advanced technologies such as microwave-assisted treatments, ultrasonic processing, and other energy-efficient methods offers a pathway to improve degumming efficiency, shorten processing times, and minimize reagent consumption. Such innovations can further enhance the scalability, eco-friendliness, and economic viability of PALF extraction and processing.

CRediT authorship contribution statement

Puwang LI: Validation, Resources, Methodology. **Xungai Wang:** Writing – review & editing, Supervision, Resources, Project administration, Methodology, Formal analysis, Conceptualization. **Shiyu LIAO:** Writing – original draft, Methodology, Investigation, Data curation, Conceptualization. **Jianming CHEN:** Writing – review & editing, Supervision, Formal analysis, Data curation. **Li LI:** Resources, Conceptualization.

Declaration of Competing Interest

The authors declare that they have no known competing financial interests or personal relationships that could have appeared to influence the work reported in this paper.

Acknowledgment

The authors acknowledge the pineapple leaf material support from the pineapple planting base of the South Subtropical Crops Research Institute, CATAS.

Data availability

Data will be made available on request.

References

Abdelwahab, N., Shukry, N., 2015. Synthesis, characterization and antimicrobial properties of grafted sugarcane bagasse/silver nanocomposites. Carbohydr. Polym. 115, 276–284. https://doi.org/10.1016/j.carbpol.2014.08.052.

Ali, M.A.-S., Abdel-Moein, N.M., Owis, A.S., Ahmed, S.E., Hanafy, E.A., 2024. Eco-friendly lignin nanoparticles as antioxidant and antimicrobial material for enhanced textile production. Sci. Rep. 14 (1), 17470. https://doi.org/10.1038/s41598-024-67449-0.

Balbin, D.J., Padilla, D., Retamal, J.B., Abana, E., Ventura, J., 2022. PALFNet: a soil erosion control geotextile using pineapple leaf fiber. Int. Conf. Struct. Eng. Constr. Manag. https://doi.org/10.1007/978-3-031-12011-4_1.

Célino, A., Fréour, S., Jacquemin, F., Casari, P., 2013. Characterization and modeling of the moisture diffusion behavior of natural fibers. J. Appl. Polym. Sci. 130 (1), 297–306. https://doi.org/10.1002/app.39148.

Choudhury, A., 2006. Textile preparation and dyeing. Science Publishers.

Choudhury, A.R., 2011. Pre-treatment and preparation of textile materials prior to dyeing. Handbook of Textile and Industrial Dyeing. Elsevier, pp. 64–149. https://doi.org/10.1533/9780857093974.1.64.

Dey, P., Mahapatra, B., Pramanick, B., Kumar, A., Negi, M., Paul, J., Shukla, D., Singh, S., 2021. Quality optimization of flax fibre through durational management of water retting technology under sub-tropical climate. Ind. Crops Prod. 162, 113277. https://doi.org/10.1016/j.indcrop.2021.113277.

Fan, X.S., Liu, Z.W., Liu, Z.T., Lu, J., 2010. A novel chemical degumming process for ramie bast fiber. Text. Res. J. 80 (19), 2046–2051. https://doi.org/10.1177/0040517510373632.

Fareez, I.M., Ibrahim, N.A., Wan Yaacob, W.M.H., Mamat Razali, N.A., Jasni, A.H., Abdul Aziz, F., 2018. Characteristics of cellulose extracted from Josapine pineapple leaf fibre after alkali treatment followed by extensive bleaching. Cellulose 25, 4407–4421. https://doi.org/10.1007/s10570-018-1878-0.

Fibre2Fashion. 2024. Average price of scutched flax fiber in China's import market from 2019 to 1st quarter of 2024 (in U.S. Dollars per Kilogram). ⟨https://www-statista-com.ezproxy.lb.polyu.edu.hk/statistics/1469533/china-scutched-flax-fiber-import-price/⟩. (accessed 24 Apr 2024).

Foulk, J.A., Mcalister III, D.D., 2002. Single cotton fiber properties of low, ideal, and high micronaire values. Text. Res. J. 72 (10), 885–891. https://doi.org/10.1177/004051750207201006.

Franck, R.R., 2005. Bast and other plant fibres (Vol. 39). Crc Press. https://doi.org/10.1533/9781845690618.

Furse, S., Egmond, M.R., Killian, J.A., 2015. Isolation of lipids from biological samples. Mol. Membr. Biol. 32 (3), 55–64. https://doi.org/10.3109/09687688.2015.1050468.

Grumo, J., Jabber, L., Patricio, J., Magdadaro, M., Lubguban, A., Alguno, A., 2017. Alkali and bleach treatment of the extracted cellulose from pineapple (Ananas comosus) leaves. J. Fundam. Appl. Sci. 9 (7S), 124–133.

Huang, T., Zhang, J., Li, M.F., Lian, W.W., He, J.Y., Zhuang, Z.K., Peng, Z., Liu, X.Y., 2014. Adhesive content influence on antimicrobial properties of pineapple leaf fiber. Adv. Mater. Res. 1048, 3–8. https://doi.org/10.4028/www.scientific.net/AMR.1048.3.

Indra Doraiswamy, I.D., Chellamani, P., 1993. Pineapple-leaf Fibres. https://doi.org/10.5555/19940307777.

Ivanovska, A., Asanovic, K., Jankoska, M., Mihajlovski, K., Pavun, L., Kostic, M., 2020. Multifunctional jute fabrics obtained by different chemical modifications. Cellulose 27, 8485–8502.

Jakob, M., Mahendran, A.R., Gindl-Altmutter, W., Bliem, P., Konnerth, J., Mueller, U., Veigel, S., 2022. The strength and stiffness of oriented wood and cellulose-fibre materials: a review. Prog. Mater. Sci. 125, 100916. https://doi.org/10.1016/j.pmatsci.2021.100916.

Kengkhetkit, N., Amornsakchai, T., 2014. A new approach to "Greening" plastic composites using pineapple leaf waste for performance and cost effectiveness. Mater. Des. 55, 292–299. https://doi.org/10.1016/j.matdes.2013.10.005.

Lee, C., Khalina, A., Lee, S., Padzil, F., Ainun, Z., 2020. Physical, morphological, structural, thermal and mechanical properties of pineapple leaf fibers. Pineapple Leaf Fiber.: Process. Prop. Appl. 91–121. https://doi.org/10.1007/978-981-15-1416-6_6.

Li, M., Han, G., Chen, H., Yu, J., Zhang, Y., 2012. Chemical compounds and antimicrobial activity of volatile oils from bast and fibers of Apocynum venetum. Fibers Polym. 13, 322–328. https://doi.org/10.1007/s12221-012-0322-6.

Li, J., Liu, X., Zheng, Q., Chen, L., Huang, L., Ni, Y., Ouyang, X., 2019. Urea/NaOH system for enhancing the removal of hemicellulose from cellulosic fibers. Cellulose 26, 6393–6400. https://doi.org/10.1007/s10570-019-02587-7.

Liu, L., Levin, M.J., Klimscha, F., Rosenberg, D., 2022. The earliest cotton fibers and Pan-regional contacts in the Near East. Front. Plant Sci. 13, 1045554. https://doi.org/10.3389/fpls.2022.1045554.

Liu, B., Qin, C., Zhang, F., Wang, S., Liang, C., Nie, S., Wang, S., Yao, S., 2020. Reaction mechanism of phenolic lignin and high concentration chlorine dioxide and its application. ACS Omega 5 (35), 22475–22481. https://doi.org/10.1021/acsomega.0c03028.

Liu, S., Wu, Q., Zhu, Z., Lin, W., Wei, C., Zhang, X., 2024. Volatile compounds of fresh pineapple (Ananas comosus cv. Josapine) in different harvest periods. BIO Web Conf. https://doi.org/10.1051/bioconf/202412401021.

Mishra, S., Mohanty, A.K., Drzal, L.T., Misra, M., Hinrichsen, G., 2004. A review on pineapple leaf fibers, sisal fibers and their biocomposites. Macromol. Mater. Eng. 289 (11), 955–974. https://doi.org/10.1002/mame.200400132.

Mukherjee, P., Satyanarayana, K., 1986. Structure and properties of some vegetable fibres: part 2 Pineapple fibre (Anannus comosus). J. Mater. Sci. 21, 51–56.

Neto, A.R.S., Araujo, M.A., Barboza, R.M., Fonseca, A.S., Tonoli, G.H., Souza, F.V., Mattoso, L.H., Marconcini, J.M., 2015. Comparative study of 12 pineapple leaf fiber varieties for use as mechanical reinforcement in polymer composites. Ind. Crops Prod. 64, 68–78. https://doi.org/10.1016/j.indcrop.2014.10.042.

Österberg, M., Sipponen, M.H., Mattos, B.D., Rojas, O.J., 2020. Spherical lignin particles: a review on their sustainability and applications. Green. Chem. 22 (9), 2712–2733. https://doi.org/10.1039/D0GC00096E.

Padzil, F., Ainun, Z., Abu Kassim, N., Lee, S., Lee, C., Ariffin, H., Zainudin, E.S., 2020. Chemical, physical and biological treatments of pineapple leaf fibres. Pineapple Leaf Fiber.: Process. Prop. Appl. 73–90. https://doi.org/10.1007/978-981-15-1416-6_5.

Prang Rocky, B., Thompson, A.J., 2021. Investigation and comparison of antibacterial property of bamboo plants, natural bamboo fibers and commercial bamboo viscose textiles. J. Text. Inst. 112 (7), 1159–1170. https://doi.org/10.1080/00405000.2020.1807300.

Ramesh, M., 2016. Kenaf (Hibiscus cannabinus L.) fibre based bio-materials: a review on processing and properties. Prog. Mater. Sci. 78, 1–92. https://doi.org/10.1016/j.pmatsci.2015.11.001.

Reddy, B.S., Rajesh, M., Sudhakar, E., Rahaman, A., Kandasamy, J., Sultan, M., 2020. Pineapple leaf fibres for automotive applications. Pineapple Leaf Fiber.: Process., Prop. Appl. 279–296. https://doi.org/10.1007/978-981-15-1416-6_14.

Sethupathi, M., Khumalo, M.V., Skosana, S.J., Muniyasamy, S., 2024. Recent developments of pineapple leaf fiber (PALF) utilization in the polymer composites—a review. Separations 11 (8), 245. https://doi.org/10.3390/separations11080245.

Sjostrom, E., 2013. Wood chemistry: Fundamentals and applications. Elsevier.

Taylor, S., 2012. The chemistry and technology of pectin. Academic Press. https://doi.org/10.1016/C2009-0-02630-0.

Thakur, B.R., Singh, R.K., Handa, A.K., Rao, M., 1997. Chemistry and uses of pectin—a review. Crit. Rev. Food Sci. Nutr. 37 (1), 47–73. https://doi.org/10.1080/10408399709527767.

Tian, Y., Liu, X., Zheng, X., Wang, L., 2016. Antimicrobial properties of flax fibers in the enzyme retting process. Fibres Text. East. Eur. 24 (1 (115), 15–17. https://doi.org/10.5604/12303666.1172082.

Todhanakasem, T., Panjapiyakul, S., Koombhongse, P., 2022. Novel pineapple leaf fibre composites coating with antimicrobial compound as a potential food packaging. Packag. Technol. Sci. 35 (1), 97–105. https://doi.org/10.1002/pts.2612.

Triastuti, W.E. 2021. Effect of alkali treatment on processing of pineapple leaf fibers. AIP Conference Proceedings. https://doi.org/10.1063/5.0045348.

Trivedi, A.K., Gupta, M., 2023. An efficient approach to extract nanocrystalline cellulose from sisal fibers: structural, morphological, thermal and antibacterial analysis. Int. J. Biol. Macromol. 233, 123496. https://doi.org/10.1016/j.ijbiomac.2023.123496.

Wan, J., Wang, Y., Xiao, Q., 2010. Effects of hemicellulose removal on cellulose fiber structure and recycling characteristics of eucalyptus pulp. Bioresour. Technol. 101 (12), 4577–4583. https://doi.org/10.1016/j.biortech.2010.01.026.

Wei, C., Xiong, S., Zhang, S., Cui, Y., Wang, S., Lu, X., Chen, J., Zhang, M., Yang, B., 2023. A study on the antibacterial property and biocompatibility of ramie fiber. Biomed. Mater. 18 (4), 045010. https://doi.org/10.1088/1748-605X/acd49c.

Xi, L., Qin, D., An, X., Wang, G., 2013. Resistance of natural bamboo fiber to microorganisms and factors that may affect such resistance. BioResources 8 (4), 6501–6509. https://doi.org/10.5555/20133400856.

Xiang, Y., Yu, J., Liu, L., Zhang, R., Qu, Y., Jing, M., 2019. The chemo-enzymatic modification and degumming of hemp fiber by the laccase-2, 2, 6, 6-tetramethylpiperidine-1-oxyl radical-hemicellulase system and physico-chemical properties of the products. Text. Res. J. 89 (12), 2433–2443. https://doi.org/10.1177/0040517518792724.

Yang, H., Zhang, Y., 1999. Tentative research of hemp fast chemical degumming. J. China Text. Univ. 25 (5), 83–86.

Zakaria, Z., Zakaria, M., Amom, Z., Desa, M., 2011. Antimicrobial activity of the aqueous extract of selected Malaysian herbs. Afr. J. Microbiol. Res. 5 (30), 5379–5383. https://doi.org/10.5897/AJMR11.874.

Zamora-Mendoza, L., Guamba, E., Miño, K., Romero, M.P., Levoyer, A., Alvarez-Barreto, J.F., Machado, A., Alexis, F., 2022. Antimicrobial properties of plant fibers. Molecules 27 (22), 7999. https://doi.org/10.3390/molecules27227999.